The role of specific cations and water entropy on the stability of branched DNA motif structures

Tod A Pascal, William A Goddard III, Prabal K Maiti and Nagarajan Vaidehi

Supporting Information

1. Figures

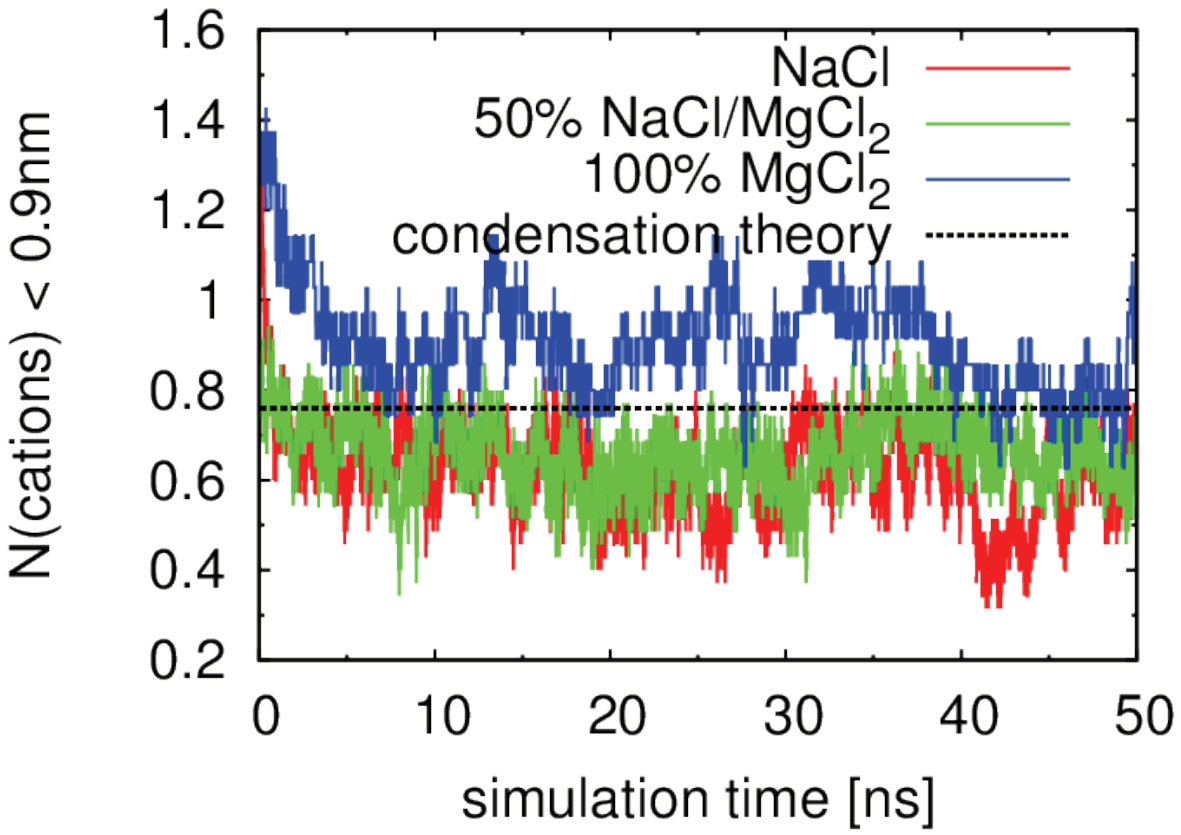

Figure S1. Time evolution of the fraction of ions within 0.9nm of TWJ1 surface during MD. The results of all 3 of our simulations as well as the prediction (0.78) of counterion condensation theory (dashed line) are shown. In the case of our simulations, convergence is observed after 25ns.

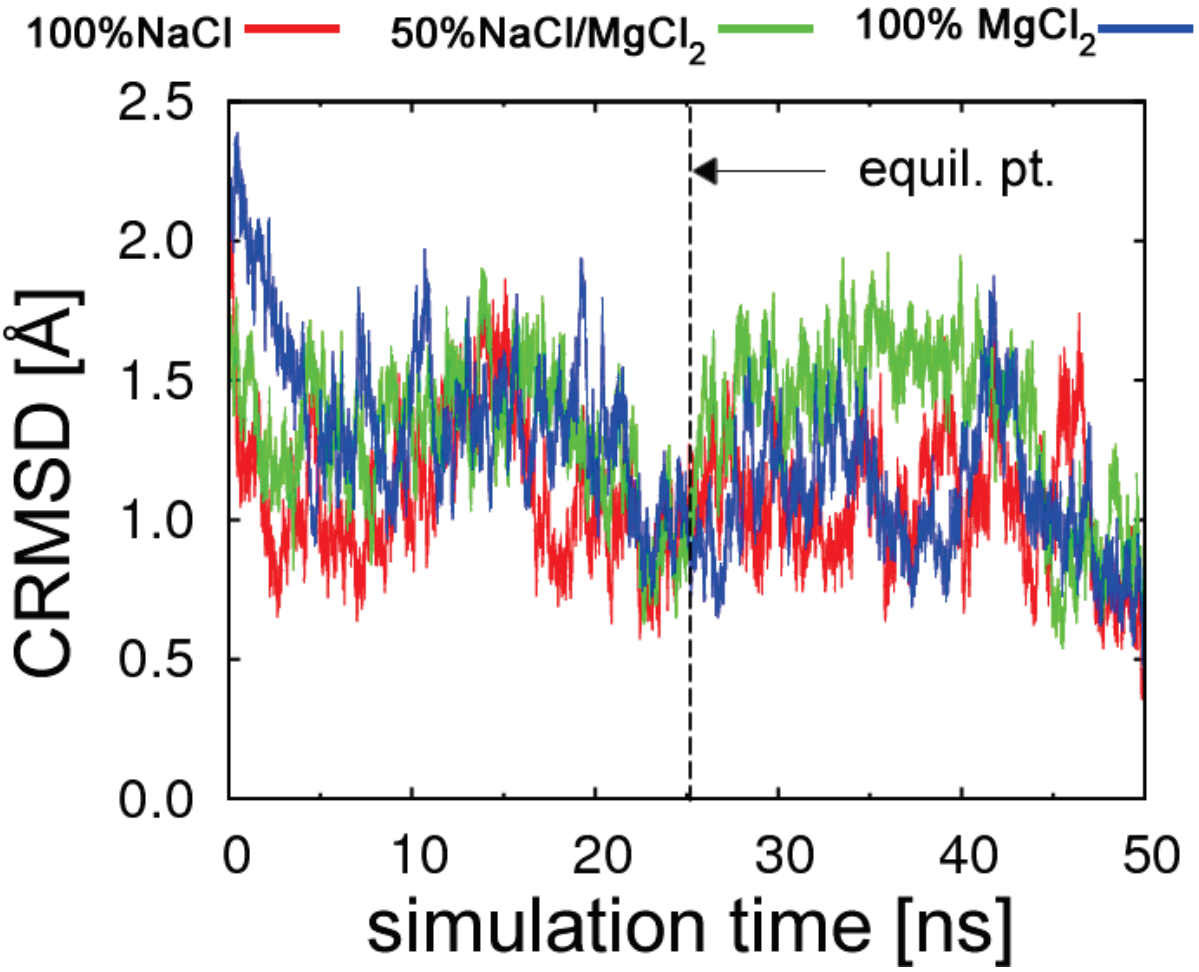

Figure S2. Coordinate root mean square deviation of TWJ1 in 100% NaCl (red), 50% $NaCl/MgCl_2$ (green) and 100% $MgCl_2$ (blue) relative to the average MD structure. The simulations converge to 1.56±0.34, 2.03±0.46 and 1.60±0.35 Å respectively after ~25 ns (vertical dashed line)

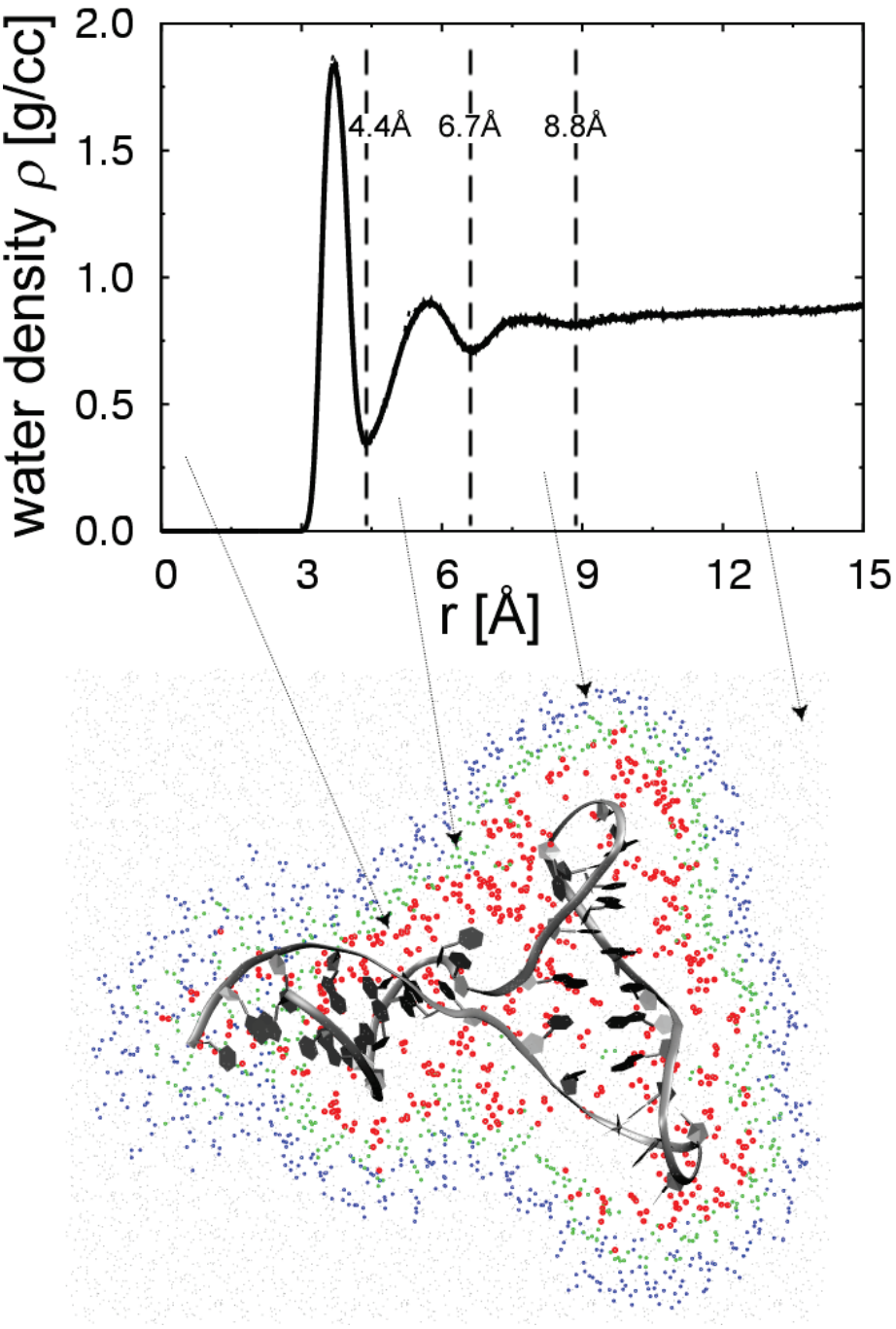

Figure S3. a) PO_4^{2-} - water (oxygen atom) radial distribution function (RDF) for TWJ1 during dynamics. The RDFs were measured during the last 25ns of the 50ns MD trajectory. The RDFs of each of the 3 simulations are virtually identical. The various hydration shells are characterized by valley – valley distances in the RDF. So the locations of the solvation shells are 4.4, 6.7, 8.8 and 11.0 Å for the 4 hydration shells. These are indicated by considering the final snapshot of the TWJ1 in 100% NaCl structure, where the 1st shell (red), 2nd shell (green) and 3rd shell (blue) are shown.

2. Tables.

Table S1. Van der Waals (vdW) parameters and fixed charges for water and ions used in this study. All parameters not specified are obtained using geometric combination rules.

i	j	Charge (e-)	ε (kJ/mol)	σ (Å)
[a]**Water (SPC/E)**	Water	Oxygen (Ow): -0.82, Hydogen (Hw): +0.41	Ow: 0.636 Hw: 0.0	Ow: 3.15 Hw: 0.0
[b]**Na^+**	Na^+	+1	1.475	2.424
[c]**Mg^{2+}**	Mg^{2+}	+2		
[b]**Cl^-**	Cl^-	-1	0.0535	5.422

Table S2. Average population of ions and water in the TWJ1 hydration shells from the last 25ns of 50ns MD simulations.

		Shell1 (0 – 4.5Å)	Shell2 (4.6 – 6.6Å)	Shell3 (6.7 – 8.8Å)	Shell4 (8.9 – 11.0Å)	Bulk (> 11.1 Å)
100% NaCl	water	284	434	502	584	6523
	Na^+	5.4	9.6	5.0	6.9	23.1
	Cl^-	0.2	0.3	0.5	0.8	13.2
50% NaCl/ $MgCl_2$	water	296	443	523	626	6439
	Na^+	3.3	4.3	3.8	3.2	20.4
	Mg^{2+}	1.7	3.4	0.8	1.3	0.8
	Cl^-	0.2	0.3	0.6	0.9	13.0
100% $MgCl_2$	water	301	439	504	601	6482
	Mg^{2+}	6.3	7.2	2.0	1.4	8.1
	Cl^-	0.1	0.4	0.7	1.0	12.8

Table S3. Thermodynamics of TWJ1 systems

Pure NaCl								
	nmol		**<G> kJ/mol**		**<H> kJ/mol**		**<S> J/mol/K**	
	avg	std	Avg	std	avg	std	avg	std
Shell1	284	15	-53.8	0.1	-36.3	0.1	58.7	0.5
Shell2	434	20	-53.9	0.1	-34.0	0.1	67.0	0.4
Shell3	502	26	-54.1	0.1	-34.7	0.1	65.2	0.3
Shell4	584	29	-54.1	0.1	-34.6	0.1	65.4	0.3
Bulk	6523	50	-54.0	0.0	-34.5	0.0	65.5	0.2
DNA	1		-25055.0	89.1	-21890.1	103.5	10807.1	85.7
Na^+	50		-405.7	0.9	-392.8	0.8	43.1	0.9
Cl^-	15		-392.9	1.1	-373.4	0.9	65.0	2.0
50% $NaCl/MgCl_2$								
Shell1	296	17	-55.5	0.2	-38.2	0.2	58.0	0.5
Shell2	443	19	-55.2	0.2	-35.0	0.2	67.7	0.4
Shell3	523	25	-54.2	0.1	-34.8	0.2	65.1	0.3
Shell4	626	32	-54.1	0.1	-34.6	0.1	65.3	0.3
Bulk	6439	50	-54.0	0.0	-34.5	0.0	65.3	0.2
DNA	1		-26829.2	97.4	-23642.1	111.8	10873.5	89.1
Na^+	34		-406.4	0.8	-393.0	0.8	44.5	1.1
Cl^-	15		-392.7	1.0	-373.2	1.0	65.2	1.9
Mg^{2+}	8		-1629.4	2.4	-1622.0	2.3	24.9	1.5
Pure $MgCl_2$								
Shell1	301	16	-58.3	0.4	-42.2	0.4	54.1	0.5
Shell2	439	19	-57.2	0.3	-37.5	0.3	66.1	0.4
Shell3	504	24	-55.3	0.2	-36.8	0.3	61.9	0.4
Shell4	601	25	-55.1	0.2	-36.5	0.2	62.3	0.3
Bulk	6482	38	-55.0	0.1	-36.4	0.1	62.5	0.2
DNA	1		-24301.2	93.9	-21226.0	105.9	10502.4	88.9
Mg^{2+}	25		-1650.5	1.6	-1642.9	1.6	25.3	0.9
Cl^-	15		-393.8	1.0	-375.1	1.0	62.5	1.8

Table S4. Analysis of rotational (Srot) and translational (Strans) water entropy (J/mol/K) in various solvation shells around TWJ1.

	pure NaCl		**50% NaCl/$MgCl_2$**		**pure $MgCl_2$**	
	avg	std	avg	std	avg	std
Srot						
Shell 1	9.89	0.10	9.68	0.10	8.93	0.10
Shell 2	12.48	0.09	12.39	0.09	12.61	0.08
Shell 3	10.54	0.08	10.50	0.08	9.78	0.07
Shell 4	10.54	0.06	10.50	0.07	9.81	0.07
Bulk	10.53	0.04	10.51	0.05	9.81	0.04
Water box[a]	10.41	0.04				
Strans						
Shell 1	48.76	0.45	48.27	0.43	45.15	0.44
Shell 2	54.48	0.33	55.27	0.35	53.51	0.34
Shell 3	54.67	0.30	54.56	0.30	52.15	0.31
Shell 4	54.90	0.27	54.77	0.27	52.53	0.28
Bulk	54.99	0.14	54.81	0.13	52.67	0.14
Water box	49.87	0.14				

[a]Reference [1]

3. Methods

Estimating of the system thermodynamics from MD simulations

3.a.i. Solids: Debye theory of solids

The canonical partition function Q of a system is related to the entropy S, internal energy E, Helmholtz free energy A and constant volume heat capacity C_v by[2]

$$S = k_B T \frac{\partial \ln Q}{\partial T} + k_B \ln Q \qquad (1)$$

$$E = k_B T^2 \frac{\partial \ln Q}{\partial T}$$

$$A = E - TS = -k_B T \ln Q$$

$$C_v = \frac{\partial E}{\partial T}$$

where k_B is Boltzmann's constant. In the harmonic limit, one approximates the normal modes of a system as a set of 3N harmonic oscillators, so that the partition function Q can be expressed in term of the partition function q_i for the individual modes[3]:

$$Q = \prod_{i=1}^{3N} q_i \qquad (2.1)$$

or

$$\ln Q = \sum_{i=1}^{3N} q_i \qquad (2.2)$$

and for a continuous distribution of normal frequencies

$$\ln Q = \int_0^{\infty} DoS(v) \ln q(v)\, dv \qquad (2.3)$$

where *DoS(v)* is the density of states function at frequency *v*. The *DoS(v)* can be extracted directly from a MD trajectory as the Fourier transform of the integrated atomic velocity autocorrelation function (VACF) *C(t)*:

$$DoS(v) = \lim_{\tau \to \infty} \frac{1}{2kT} \int_{-\tau}^{\tau} C(t) \exp(-2\pi v t)\, dt \qquad (3.1)$$

where

$$C(t) = \sum_{i=1}^{N} \sum_{j=1}^{3} m_i \left[\lim_{\tau \to \infty} \frac{1}{2\tau} \int_{-\tau}^{\tau} v_i^j(t'+t)\, v_i^j(t)\, dt' \right] \qquad (3.2)$$

m_i is the mass and $v_i^j(t)$ is the j-th component of the velocity of atom i at time t. Thus all that remains to extract the thermodynamics in eqn (1) is the weighting function $q(v)$ in 2.3, which becomes that of a quantum harmonic oscillator[2]

$$q(v) = \frac{\exp(-\beta hv/2)}{1-\exp(-\beta hv)} \qquad (4)$$

where $\beta = 1/k_B T$ is the energy of the harmonic oscillator at temperature T.

2.a.ii. Gases: Carnahan-Starling hard sphere

For a hard-sphere gas of N particles at constant pressure P and temperature T, the VACF decays exponentially[2]

$$C^{gas}(t) = C^{gas}(0)\exp(-\alpha t) = \frac{3kT}{m}\exp(-\alpha t) \qquad (5.1)$$

and

$$DoS(v) = \frac{4}{kT}\int_0^\infty 3NkT\exp(-\alpha t)\cos(2\pi vt)\,dt \qquad (5.2)$$

where α is the Enskog friction constant related to the collisions between hard spheres. The absolute thermodynamics can then be obtained from integrating (5.2) with the appropriate weighting functions:

$$W_E = C_v = 0.5 \qquad (6)$$

$$W_S = \frac{S^{gas}}{3k_B}$$

$$W_A = E - TS = \frac{1.5k_B - TS^{gas}}{3k_B}$$

where S^{gas} can be obtained from the accurate Carnahan–Starling equation of state[4]:

$$S^{gas} = k_B\left\{\ln\left[z(y)\right] + \frac{y(3y-4)}{(1-y)^2}\right\} \qquad (7)$$

$$z(y) = \frac{1+y+y^2-y^3}{(1-y)^3}$$

where y is the hard-sphere packing fraction defined as $y = \pi\rho\sigma^3/6$.

3.a.iii. Liquids: 2PT method for condensed phase systems

By inspection, one observes that substituting eqn (4) into (2.3) results in a singularity at $v = 0$ for a finite $DoS(0)$. While a $DoS(0) = 0$ for a solid, in a liquid and generally for strongly interacting systems, $DoS(0) > 0$ due to diffusion

$$DoS(0) = \frac{12mND}{k_B T} \qquad (8)$$

where D is the self-diffusion constant. One method of addressing this issue is the Two-Phase Thermodynamics (2PT) method[1,5] which is based on the Lin, Blanco and Goddard (LBG) theory of condensed phase thermodynamics. The 2PT method builds on an idea first proposed by Eyring and Rae[6] whereby the DoS function of a liquid is expressed as a linear combination of a gas (eqn 5.2) and a solid (eqn 2.3):

$$DoS_{tot}(v) = fDoS_{gas}(v) + (1-f)DoS_{solid}(v) \qquad (9)$$

where f, termed the "fluidicity" factor, is the number of diffusive modes in the system. Thus as implemented in 2PT, LGB showed that by setting $DoS_{tot}(0) = DoS_{gas}(0)$, $DoS_{solid}(0) = 0$, the singularity in eqn 4 is avoided and the thermodynamics obtained by integrating with the appropriate weighting functions in eqn 1 and 6. All that remained is to define the f factor. Thus a defining feature of LBG theory is that f can be determined self-consistently from the MD trajectory

$$DoS_{tot}(0) = DoS_{gas}(0) = \frac{12fN}{\alpha} \qquad (10.1)$$

since f is related to the packing fraction y by[1]

$$2y^3 f^3 - (y + 6y^2) f^2 + (2 + 6y) f - 2 = 0 \qquad (10.2)$$

3.b. Application to real systems

For strongly coupled system such as liquids, there are quantifiable differences in the zero-point energy motions, enthalpy and heat capacity of the system described quantum-mechanically (with discrete energy states) and classically (with a continuum of states), where the quantum description being closer to the experimental reality. These quantum effects are especially important in accurately describing the physics of water[7], even at room temperature where one would expect the effect to by minimal[8]. In lieu of performing prohibitive quantum dynamics, one can approximate the quantum effects from classical trajectories by Feyman-Hibbs[9] path integral techniques[10], or by the Wigner-Kirkwod technique[11,12] of adding the first term in the power series expansion of the energy in h^2 to the classical values. An alternative approached introduced by Berens et al[3] approximates the quantum effects as the difference in the DoS using the weighting function of the quantum harmonic oscillator in Eqn. 4 and the classical harmonic oscillator $q^C(v) = (\beta h v)^{-1}$. Thus in addition to providing an efficient estimate of the quantum molar entropy, the 2PT method allows for the approximation of quantum effects in the internal energy U:

$$U \approx E_{pot} + E_{kin} + \Delta U_{Q->C} \quad (11.1)$$

where E_{pot} is the potential energy, E_{kin} is the kinetic energy and $\Delta U_{Q\to C}$ is the quantum correction, and the constant volume heat capacity C_v

$$C_v = \left(\frac{\partial E}{\partial T}\right)_{N,V,T} \approx \frac{\langle U \rangle^2 - \langle U^2 \rangle}{N k_b \langle T \rangle^2} + \Delta C v_{Q->C} \quad (11.2)$$

where the < > brackets is indicates the statistical average, $<U>^2$-$<U^2>$ is the variance, and $\Delta Cv_{Q\to C}$ is the quantum correction.

4. References

(1) Lin, S. T.; Maiti, P. K.; Goddard, W. A. *J. Phys. Chem. B* **2010**, *114*, 8191.

(2) McQuarrie, D. A. *Statistical mechanics*; University Science Books: Sausalito (Calif.), 2000.

(3) Berens, P. H.; Mackay, D. H. J.; White, G. M.; Wilson, K. R. *J. Chem. Phys.* **1983**, *79*, 2375.

(4) Carnahan, N. F.; Starling, K. E. *J. Chem. Phys.* **1970**, *53*, 600.

(5) Lin, S. T.; Blanco, M.; Goddard, W. A. *J. Chem. Phys.* **2003**, *119*, 11792.

(6) Eyring, H.; Ree, T. *Proceedings of the National Academy of Sciences* **1961**, *47*, 526.

(7) Horn, H. W.; Swope, W. C.; Pitera, J. W.; Madura, J. D.; Dick, T. J.; Hura, G. L.; Head-Gordon, T. *The Journal of Chemical Physics* **2004**, *120*, 9665.

(8) Vega, C.; Conde, M. M.; McBride, C.; Abascal, J. L. F.; Noya, E. G.; Ramirez, R.; Sese, L. M. *The Journal of Chemical Physics* **2010**, *132*, 046101.

(9) Feynman, R. P.; Hibbs, A. R. *Quantum mechanics and path integrals*; McGraw-Hill: New York, 1965.

(10) Doll, J. D.; Myers, L. E. *The Journal of Chemical Physics* **1979**, *71*, 2880.

(11) Wigner, E. *Physical Review* **1932**, *40*, 749.

(12) Kirkwood, J. G. *Physical Review* **1933**, *44*, 31.